Plasticized/Graphite Reinforced Phenolic Resin Composites and Their Application Potential

Farid El-Tantawy

Department of Physics, Faculty of Science, Suez Canal University, Ismailia, Egypt

Received 25 November 2005; accepted 1 April 2006
DOI 10.1002/app.25794
Published online in Wiley InterScience (www.interscience.wiley.com).

ABSTRACT: Plasticized graphite (PG)/phenolic resin composites are candidates for positive temperature coefficient resistivity (PTCρ) thermistors, which are used for self-recoverable elements that provide protection from overcurrents, gasoline sensors, and electrostatic charge and electromagnetic wave shielding in many kinds of electrical devices. The morphology and network structure of PG/phenolic resin composites have been characterized with scanning electron microscopy and with measurements of the crosslinking density, bound resin content, degree of crystallinity, viscosity, surface energy, thermal conductivity, enthalpy, and glass-transition temperature. In addition, mechanical properties such as the tensile strength, Young's modulus, Shore A hardness, and elongation at break for resins filled with PG have been studied. The electrical properties of the composites have been measured to relate the PG volume fraction to the electrical conductivity. A large PTCρ value has been observed for all samples. The mechanism of the PTCρ effect in the materials is related to the thermal expansion and highest barrier energy of the composites. Switching behaviors of the current and voltage for all samples have been observed. The applicability of PG/phenolic resin composites for temperature controllers and gasoline gas sensors has been examined. The antistatic charge dissipation and dielectric constant as functions of the PG content have been studied. Finally, the experimental electromagnetic interference of the PG/phenolic composites has been investigated in the frequency range of 1–15 GHz and compared with a theoretical model. © 2007 Wiley Periodicals, Inc. J Appl Polym Sci 104: 697–709, 2007

Key words: composites; conducting polymers; interpenetrating networks (IPN); resins; sensors

INTRODUCTION

Nowadays, conducting polymer composites are one of the main research areas because of their interesting physical properties and their various functional applications.[1,2] The increasing requests for thermistors, temperature controllers, self-heaters, gas sensors, electrostatic charge dissipation, and electromagnetic interference (EMI) shielding are pushing many researchers to explore new concepts and related materials.[3–10] Electrically conductive polymer composites (CPCs) are obtained by the blending of an insulating polymer matrix with conductive fillers such as carbon black, carbon fibers, and graphite or metal particles.[11–15] The filler loading needed for a composite is usually as high as 17 wt % to reach satisfactory conductivity; this results, however, in poor mechanical properties and high densities for the materials.[16–20] CPCs exhibit several interesting features because of their resistivity variation with thermal, mechanical, and chemical treatments. A self-regulated heating ability can be obtained for CPCs with a sharp positive temperature coefficient resistivity (PTCρ) effect.[21–25] The characterization of the electrical properties as a function of temperature is, in this case, essential for heating-device design. Changing the nature of the PTCρ effect, transition temperature, and amplitude allows the adjustment of the properties of the CPCs, which thus reach a wider range of applications.[1] However, the increasing complexity of electronic devices and systems in the form of high packing densities and quick responses has generated pollution in the form of EMI.[26–30] Electromagnetic radiation is one of the unfortunate byproducts of the rapid proliferation of electronic devices. If this problem is left unattended, it can cause severe damage to systems and, therefore, has to be controlled. Typical metals possess very high EMI shielding but have disadvantages such as heavy weight, easy corrosion, and poor processability for shielding materials.[21–23] Although CPCs have many advantages, such as portability, low cost, easy construction of complex shapes, and superior design capabilities, they are capable of not only reflecting but also absorbing electromagnetic waves. To the best of our knowledge, no information is available on the physical properties of phenolic-resin-filled plasticized graphite (PG) composites in the open literature. In this article, we investigate the network structure and transport properties of phenolic-filled PG composites for the first time. The influence of the electrical conductivity, charge carrier mobility (μ), and thermoelectric power (TEP) on the PG content of the composites is addressed. The current–voltage charac-

Correspondence to: F. El-Tantawy (faridtantawy@yahoo.com).

Journal of Applied Polymer Science, Vol. 104, 697–709 (2007)

teristics of the composites are studied. The applicability of the composites for gasoline gas sensors, temperature controllers, and static charge dissipation is tested. Finally, the EMI properties of the resin composites are evaluated and compared with theoretical predictions.

EXPERIMENTAL

A commercially available resole-type phenolic resin (Kuk Do Chemical Industry Co., Ltd., Seoul, South Korea) was used as the insulator matrix. The conductive filler was graphite with a particle size of 2 μm and a surface area of 120 m^2/g (Tokyo Chemical Industry Co., Tokyo, Japan). Dioctyl phthalate (DOP) with a molecular weight of 390.75 g/mol was used as a plasticizer; it was purchased from Koa Chemical Co (Tokyo, Japan). First, graphite powder was ground with 13 wt % DOP for 30 min with an alumina agate ball mortar. Phenolic/PG composites with various weight ratios of graphite to phenolic resin—95/05, 90/10, 85/15, 80/20, and 75/25—were prepared and are abbreviated as PG5, PG10, PG15, PG20, and PG25, respectively. The materials and compound formulations are given in Table I. The green phenolic resin with different contents of PG was prepared with a centrifuging mixer for 2 min at room temperature. The bulk samples of the composites were obtained through the casting of the green composites on a Teflon mold. The specimens were transferred to a hot press for curing under a uniaxial pressure of 500 KN/m^2 at a temperature of 130°C for 30 min. Samples in a sheet form ($90 \times 60 \times 2$ mm^3) were obtained as a final result. The crosslinking density (CLD) was obtained by a mechanical stress–strain measurement with the following relation:[1,31]

$$\mathrm{CLD} = C_1/(\rho_c RT) \tag{1}$$

where ρ_c is the composite density, R is the universal gas constant, and T is the temperature (K). C_1 is the characteristic constant of the composites and is given by

$$F = 2A_0(\lambda - \lambda^{-2})(C_1 + C_2\lambda^{-1}) \tag{2}$$

where F is the tensile extension force required for stretching a sample, A_0 is the area of the unstretched sample, λ is identifiable with F/A_0, and C_2 is the characteristic constant of the composites.

TABLE I
Formulations of the Mixes

Ingredient	PG0	PG10	PG15	PG20	PG25
Phenolic resin (phr)	100	90	85	80	75
DOP (phr)	13	13	13	13	13
Graphite (phr)	0	10	15	20	25

The bound resin content (BR) was determined by the extraction of unbound materials such as ingredients and free resins with toluene for 72 h and with hexane for 48 h and drying in a vacuum oven at 40°C for 24 h. BR was estimated with the following formula:[1]

$$\mathrm{BR}\ (\%) = [\varpi_{fg} - \varpi_s(m_f/m_f + m_r)] / \varpi_s(m_r/m_f + m_r) \times 100 \tag{3}$$

where ϖ_{fg} is the weight of the filler and gel after extraction; ϖ_s is the weight of the specimen; and m_f and m_r are the fractions of the filler and resin in the compound, respectively.

Scanning electron microscopy (SEM) was performed on a JEOL (Tokyo, Japan) model 200 field emitting scanning microscope at an operating pressure of 10^{-5} mbar and an acceleration voltage of 30 kV. The linear thermal expansions were measured in air with a Rigaku (Tokyo, Japan) TMA8310 differential dilatometer. Differential scanning calorimetry (DSC; DSC-50, Shimadzu, Osaka, Japan) with operation software was used for the determination of some thermal properties such as the glass-transition temperature (T_g), thermal conductivity (k), and enthalpy. Approximately 2-mg samples of each composition were heated from the ambient temperature to 300°C at a scanning rate of 10°C/min in a flowing inert (argon) atmosphere. The enthalpy was determined by the DSC method according to the area of the DSC peaks and was normalized to the resin content in the composites. The T_g values were determined at the midpoint of the transition point of the heat capacity change. The degree of crystallinity (X) was determined in a second melting run after normalized crystallization at a cooling rate of 10°C/min. X of the composites was calculated from DSC with the following relation:[1,32]

$$X(\%) = \left(\frac{\Delta H_m}{\Delta H_0}\right) \times 100 \tag{4}$$

where ΔH_m is the heat of crystallization for resin composites and ΔH_0 is the degree of crystallization for a 100% crystalline resin.[7]

The viscosity (η) of green and filled resin composites was measured with a model VM-1A dynamic viscometer (Yokogawa, Tokyo, Japan). The capillary had a length-to-diameter ratio of 20.0/0.9 (mm). η was determined at a fixed frequency of 10 Hz, a static force of 0.2 N, an amplitude of 5.0 μm, and room temperature. The surface energy (γ) of the resin composites was measured with a surface tension meter (model GBYP, no. 8112, Shimatzu, Osaka, Japan). The bulk direct-current (dc) electrical conductivity (σ) of the composites was measured by the two-probe tech-

nique. The conductivity was calculated from the current–voltage characteristics measured with Keithley (New York, USA) 642 and 661 programmable electrometers, which were also used for stabilized dc power voltage ranging from 0 to 2 V. Copper electrodes were embedded into samples during the preparation process to reduce the sample–electrode contact resistance.[1] The data were automatically collected with a suitable interface and data acquisition probe-computer (pc) code. TEP was measured through a pair of copper leads attached to the sample, and a minute amount of silver paste was used to measure the thermal voltage (ΔV) with a Yokogawa (Tokyo, Japan) PO30 portable logger. The temperature difference (ΔT) was controlled with a temperature controller. TEP of the resin composites was estimated as follows:

$$\text{TEP} = \frac{\Delta V}{\Delta T}$$

The dielectric constant was measured at 1 KHz with an RLC Bridge (Hioki, Japan) 3535 Z-Hitester. The mechanical properties of the samples, such as the tensile strength (TS) and Young's modulus (YM), were determined with a mechanical testing instrument from Shimadzu. The hardness of the specimen was measured according to ASTM D 2240-78 with a Shore D durometer. The static energy (SE) of the composites was measured with an SCM-5 static charge meter (Asahi Electronics, Tokyo, Japan). SE was computed as follows:[1,5]

$$\text{SE} = 0.5 C_s V_i^2 \quad (5)$$

where C_s is the standard capacitance of the base plate and V_i is the voltage indicated on the static charge meter.

The cell used to measure the gasoline sensor is displayed in Figure 1. The kinetics of the composite film resistance changes were evaluated with a Keithly 642 digital electrometer. The gas sensitivity was defined as the ratio of the electrical resistance in air (R_a) to that in the gasoline sample (R_g). The EMI properties were determined with a Hewlett–Packard waveguide line containing a spectroanalyzer, power meter, coefficient-of-reflection meter, and coefficient-of-attenuation meter (Yokogawa, Tokyo, Japan). The measurements were carried out in the frequency range of 1.0–15 GHz. The thickness of the testing sample was about 1 mm.

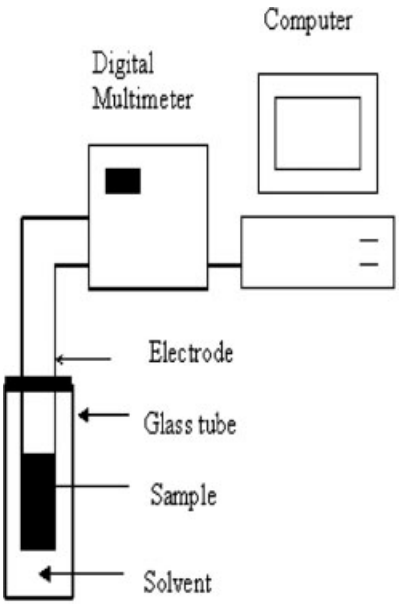

Figure 1 Cell used to measure the gasoline sensor.

RESULTS AND DISCUSSION

Composite morphology and network structure observations

Because conducting graphite/resin composites are usually applied in the field of structural materials, network structures such as the CLD, BR, k, enthalpy, and T_g are also important parameters for evaluation. To determine the effect of PG on the morphology of the phenolic composites, SEM images were first examined. Figure 2(a,b) shows the microstructures of phenolic specimens G25 (without the plasticizer) and PG25 (with the plasticizer), respectively. The G25 sample consisted of graphite particles separated by resin layers, and there was weak interfacial adhesion between the resin matrix and graphite. For sample PG25, the graphite was more dispersed, and the resin layers wrapping graphite were thicker because of larger resin molecules. Also, there was no naked graphite on the graphite surface of the samples, and this demonstrated that there existed a stronger interface between the graphite and the resin matrix. Furthermore, sample PG25 exhibited a domainlike network, and the graphite penetrated among the resin chains (i.e., located within the resin chains). This was presumably due to the longer contact area of the resin matrix with PG particles and resulted in higher CLD and BR values, as shown in Figure 3. CLD increased with an increase in the content of PG in the resin matrix. This was associated with the increase in the intermolecular forces (i.e., bonding effect) among the resin chains and graphite particles. This was supported by the fact that BR in the composites increased with increasing filler content, as shown in Figure 3. This was attributed to the fact that the free volume between the resin molecules was reduced, and this led to the increase in CLD with increasing filler content. Figure 3 shows the dependence of T_g, X, and η on the PG content for the composites. When PG was added to the composites, T_g and X increased. The

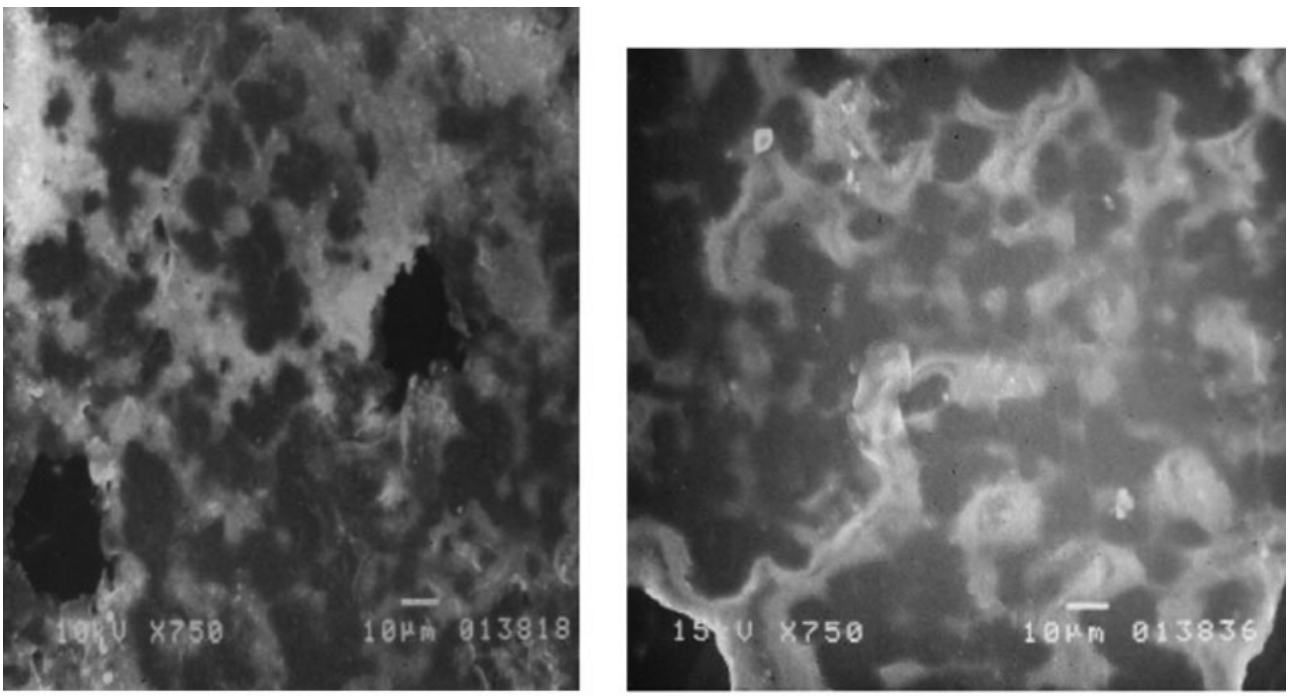

Figure 2 SEM micrographs of (a) the resin with 25 wt % graphite only (sample G25) and (b) the resin with 25 wt % PG (sample PG25).

increase in T_g and X could be attributed to the filler–resin (i.e., electron–dipole) interaction reducing the segmental motion of the resin, which in turn affected the flexibility of the composite chains and increased both X and T_g of the composites.[1,24] The increase in η could be due to the increase in the crosslinking of the composites, which reduced the flow and consequently increased η of the composites.[11] This was supported by the γ and enthalpy values of the resin composites, as shown in Figure 3. The increase in the γ and enthalpy values was due to the improved flowability of the plasticizer, which helped to make better contact between the graphite particles and resin matrix, as confirmed previously by SEM. Increasing the PG loading in the resin matrix also increased k, as shown in Figure 3. The increase could be due to the increase in the bonding force between the filler and matrix. This implied that the intermolecular force increased with increasing graphite content in the resin matrix.[26] To gain more information on the effect of the PG content on the network structure of the composites, we studied the TS, YM, Shore A hardness (H_r), and elongation at break (EBK) as functions of the graphite content, as plotted in Figure 4. TS, YM, and H_r increased with increasing loadings of PG in the composite. It is thought that a uniform dispersion of PG particles in the resin matrix and an increase in the crystallinity contributed to higher TS, YM, and H_r values for the composites. Also, we believe that the strong interfacial bonding between the graphite and phenolic resin matrix was responsible for the increases in TS, YM, and H_r of the composites. On the other hand, EBK of the resin composites decreased

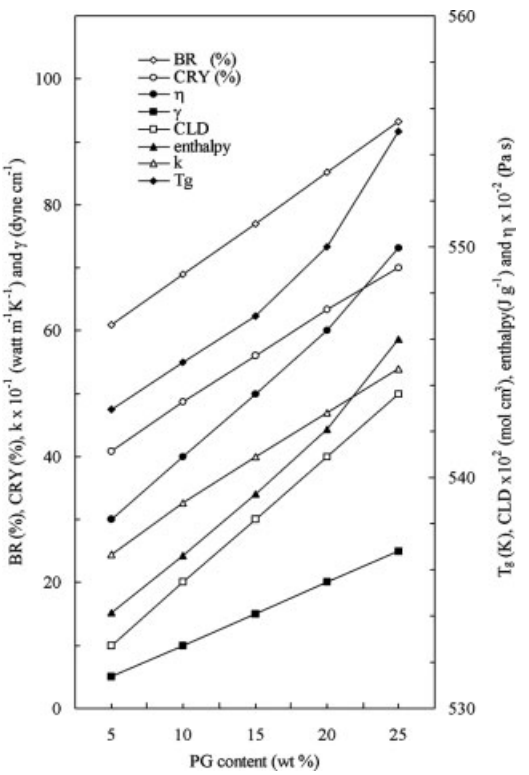

Figure 3 CLD, BR, T_g, η, γ, X, k, and enthalpy as functions of the PG content of the resin composites.

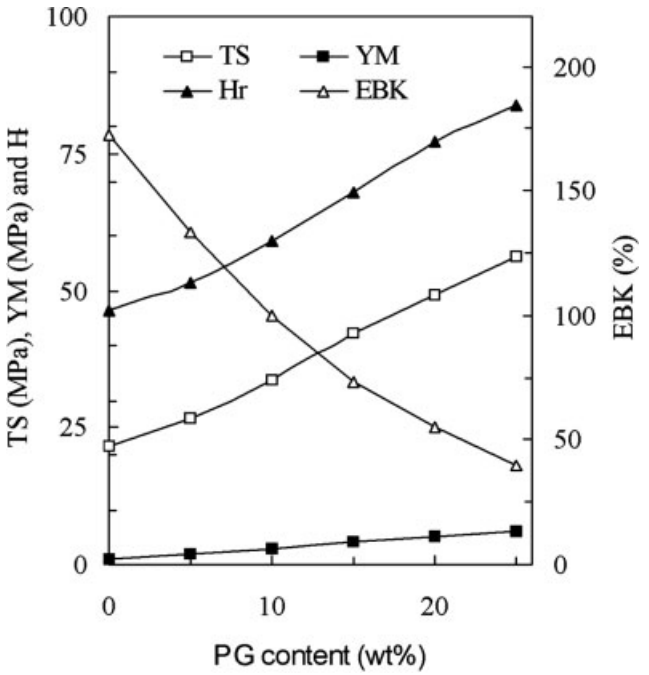

Figure 4 TS, YM, H_r, and EBK as functions of the graphite content of the composites.

with increasing PG particle loading, as shown in Figure 4. This was ascribed to the PG particles reducing the plastic flow of the resin matrix and increasing its rigidity. Thus, it was concluded that the main reason for the prominent effect on the mechanical properties was the increase in the interfacial adhesion, crystallinity, and rigidity of the resin matrix.

σ, μ, and TEP

The electrical properties of the composites depended on the nature of each of the components, their relative quantities, their distribution, the interfacial adhesion, or a combination thereof. The room-temperature electrical conductivities with the plasticizer (σ_1) and without the plasticizer (σ_2, respectively), μ, and TEP of the PG/resin composites were studied in the whole composition range, as reported in Figure 5. The level of conductivity for the graphite–plasticizer composites (i.e., σ_1) was higher than the nonmixing one (i.e., σ_2). This may be because the dispersion and interfacial adhesion of graphite grains in the phenolic matrix were considerably enhanced by the presence of the plasticizer. As a result, the plasticizer effect induced electrical conductivity because of the increase in the adhesion force between the graphite and phenolic matrix. These results indicate that the plasticizer had a noticeable effect on the dispersion behavior and the formation of the conductive filaments. However, the percolation threshold in the PG composites was about 11 wt %, whereas for the composites without DOP, it was 17 wt %. We assume that the plasticizer molecules induced the formation of a more efficient network for charge transport and by this means improved the composite conductivity; therefore, the electrical conductivity of a plasticized system should be higher, and the percolation concentration should be lower. μ increased with increasing PG particles. The charge carriers promoted the interfacial force between the graphite and phenolic matrix. This may be due to the plasticizer forming reactive chains on the grain boundary, which increased the interfacial adhesion, accelerated the diffusion of charge carriers, and increased the mobility.

However, experimental points were fitted to the scaling law from percolation theory:[1,6]

$$\sigma(\phi) = C(\phi - \phi_c)^n \quad (6)$$

where ϕ is the volume fraction of graphite, ϕ_c is the percolation threshold, C is a constant, and n is the critical exponent.

The calculated value of n for the PG resin composites was about 1.63. This result was consistent with a three-dimensional network of the conducting polymer composites.[1,27] Figure 5 shows that TEP con-

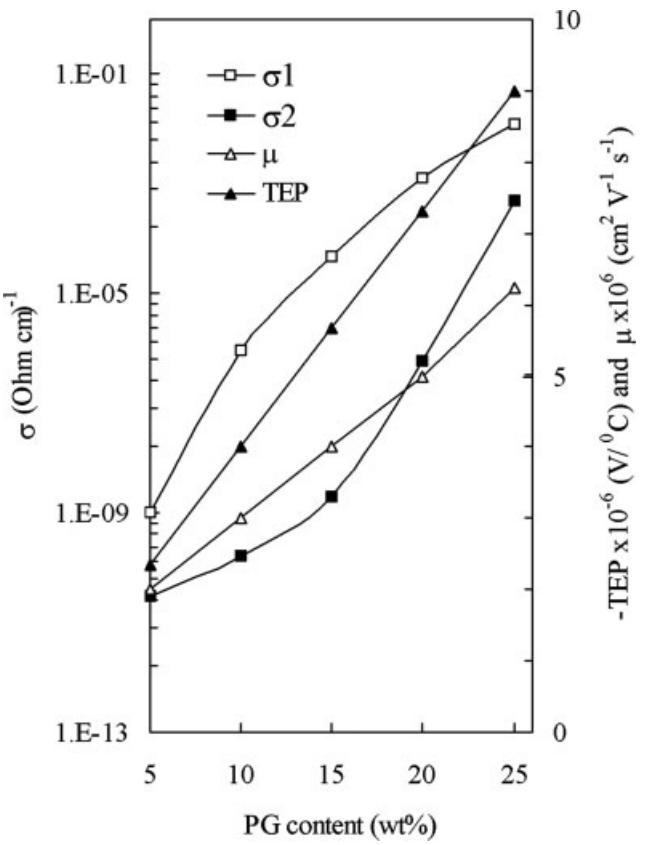

Figure 5 Dependence of σ (σ_2 for composites prepared without the plasticizer and σ_1 for composites prepared with the plasticizer), μ, and TEP of the composites as functions of the PG content.

tinuously increased with increasing PG content. The sign of TEP was negative for all tested samples. On the basis of its negative sign, the PG/resin composites were classified as *n*-type semiconductors. Thus, the conduction mechanism in the PG/resin composites was predominantly due to the hopping of electrons into the matrix, which is discussed in more detail in a later section.

Temperature dependence of the resistivity and transport mechanism

The electrical resistivity was measured to understand the transport mechanism in the composites and to understand the temperature dependence of the electrical resistivity. Figure 6(a) shows the variation of the electrical resistivity of the PG/phenolic resin composite samples with the temperature from room temperature to 150°C. All the samples exhibited strong PTCρ behaviors above a certain temperature (the peak temperature), depending on the PG content. As the PG content increased, PTCρ gradually decreased, and the peaks of the maximum resistivity shifted toward lower temperatures. As the temperature increased, the resistivity first increased slowly and then, at a peak temperature, abruptly increased. This was attributed to a lowered real graphite volume fraction (i.e., a diluted graphite composition) due to the increase in the thermal volume expansion of the phenolic resin matrix with the temperature, as shown in Figure 6(b). The other possible reason for increasing resistivity was an increasing barrier height energy (ϕ_h) with increasing temperature, as depicted in Figure 6(c), which caused an increase in the distance between the graphite and the disconnection.

Hence, ϕ_h of the composites is given by[1]

$$\phi_h = \frac{e^2 {N^2}_s}{8\varepsilon_0 \varepsilon_r N_d} \tag{7}$$

where e is the electronic charge; N_s is the interface state density; N_d is the carrier density in the grain bulk; and ε_0 and ε_r are the dielectric constants in a vacuum and air, respectively.

Electronic transport depends in general on the density of states, the position of the Fermi level, the temperature, and the applied field. The activated temperature dependence of the conductivity for the PG/resin composites followed the Mott variable-range hopping model:

$$\sigma(T) = \sigma_\infty \exp\left[-\left(\frac{T_c}{T}\right)^{1/4}\right] \tag{8}$$

where pre-exponential factor σ_∞ and characteristic temperature T_c are material-dependent constants.

σ_∞ and T_c are related to the density of localized states [$N(E_F)$] and the wavefunction decay (β) associated with these states. The characteristic Mott temperature in three dimensions can be computed as follows:[27]

$$T_c = \frac{c^4 \beta^3}{K_B N(E_F)} \tag{9}$$

where c is a number in the range of 1.85–2.30 and β is the localization radius in the range of 3–30 Å.

The range of hopping (R_h) is given by[28]

$$R_h = \frac{3}{8} {T_c}^{1/4} T^{-1/4} \left(\frac{1}{\beta}\right) \tag{10}$$

The hopping energy (w_h) is given by[29]

$$w_h = K_B (T_c T)^{1/4} \tag{11}$$

Our conductivity data fit the straight line only when ln σ values were plotted against $T^{-1/4}$. This result means that the mechanism of conductivity was three-dimensional hopping of electrons inside the resin matrix, as confirmed previously.

The activation energy (E_a) of the composite could be estimated with an Arrhenius relationship:

$$\sigma(T) = \sigma_0 \exp\left[-\frac{E_a}{K_B T}\right] \tag{12}$$

where σ_0 is the pre-exponential factor and K_B is Boltzmann's constant.

The dependence of T_c, R_h, $N(E_F)$, w_h, and E_a on the PG content for the resin composites is shown in Figure 7. T_c and R_h decreased, whereas $N(E_F)$ increased, with increasing PG content in the composites. This is a strong clue that the incorporation of PG into the resin matrix improved the quality of the molecular structure and increased μ within the resin matrix. Also, the values of w_h and E_a were not the same for the composites. These results suggest that the conduction mechanism in the PG/resin composite may be due to the hopping of electrons into the resin matrix.[1]

Current–voltage–temperature behavior

The leakage current is one of the limiting factors in PTCρ thermistor properties. Figure 8(a) presents the current as a function of voltage measured at room temperature for the PG/phenolic resin composites. The voltage was applied in 1-V steps, and the current was measured after a steady state was achieved for each voltage. Three different regions can be seen: first, in the low-voltage region below 5 V, the current was almost proportional to the applied voltage, suggest-

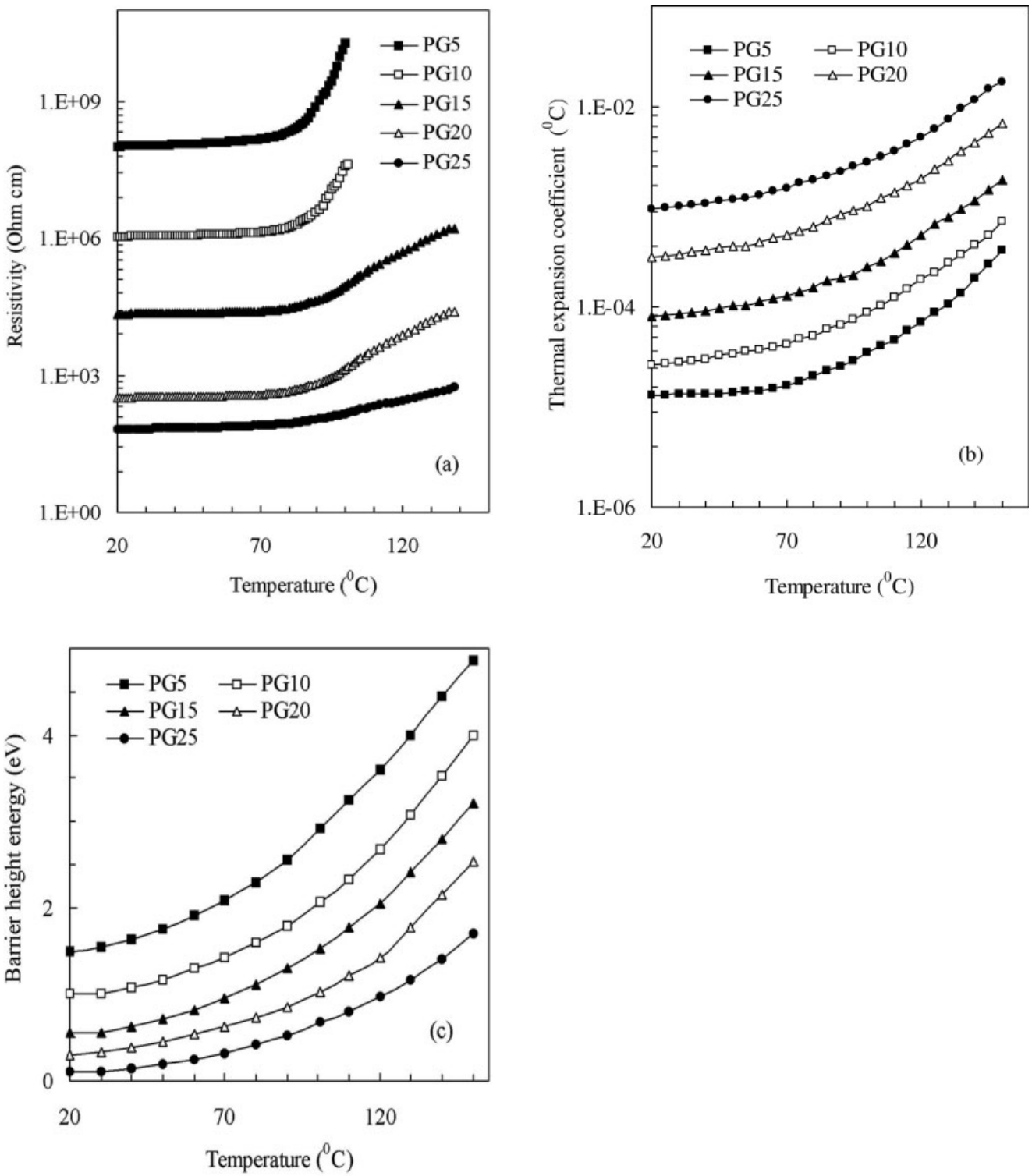

Figure 6 Temperature dependence of (a) the dc electrical resistivity, (b) the thermal expansion, and (c) the barrier height energy of the PG/resin composites.

ing ohmic conduction. Second, in the relatively high voltage region below 11 V, the current increased nonlinearly. This was attributed to the increase in the number of charge carriers at a high electric potential. Third, in the high-voltage region, the current turned up to the critical voltage (namely the switching current) and depended on the PG content. We believe that the reason for this is quite clear: at a relatively high voltage, the electrical power dissipation in the composites led necessarily to a rise in the body temperature. Therefore, the grain boundary area increased with an increase in the applied voltage. The

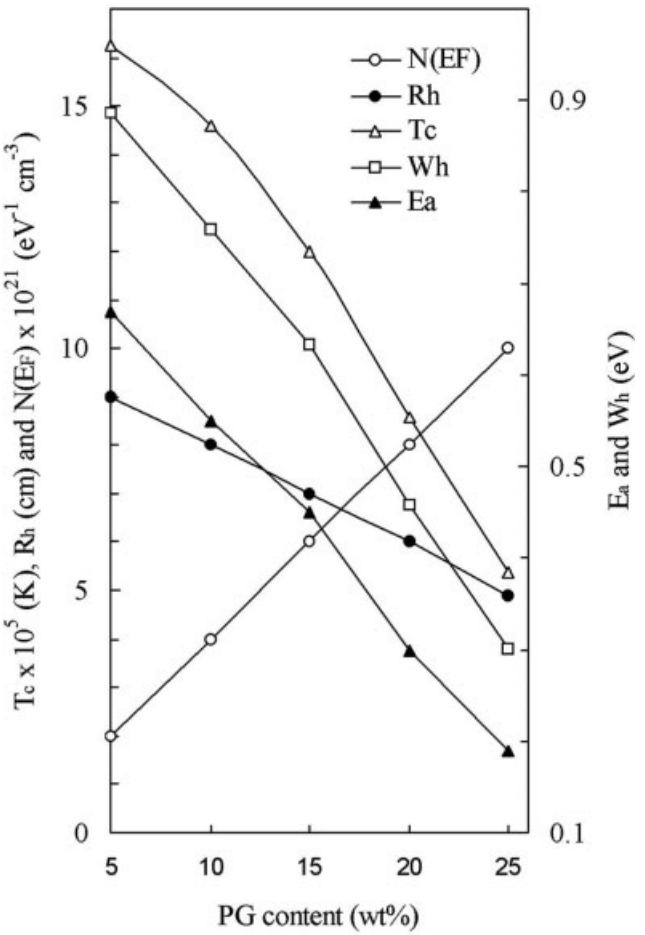

Figure 7 Dependence of T_c, R_h, $N(E_F)$, w_h, and E_a on the PG content for the resin composites.

grain boundaries acted as a scattering center of charge carriers.[1] As a result, the relative frequency of charge scattering increased, and the number of charges and μ decreased; this resulted in a decrease in the current. Accordingly, the investigated composites could be used in electronic devices as overcurrent protection. However, the current–voltage relation of a composite is given by the following equation:[30]

$$I = \left(\frac{V}{C}\right)^n \tag{13}$$

where I is the current, V is the voltage, C is the proportionality constant, and n is the nonlinear coefficient.

The current–voltage curves were plotted on a log–log scale, from which the slope of the curve gave the value of n. The computed values of n as a function of the PG content were 4, 6, 9, 13, and 18. Figure 8(b) presents the dependence of the ultimate temperature and current under an applied certain voltage for sample PG25 for two cycles (i.e., the voltage switching on and off). It is clear that the higher the volume fraction was (i.e., lower the sample resistivity was), the higher the heating rate was, and the higher the ultimate temperature was. Also, the temperature and current reached steady-state values after 300 s, and these values were satisfactory for self-heating applications. After the voltage was switched off, the temperature reached room temperature after 140 s. This reflects the fact that the PG/phenolic resin composites were quite stable at a high loading level, as confirmed previously.

Figure 8(c) shows the relationship of the maximum temperature of the bulk samples and the applied voltage for the PG/phenolic resin composites. The level of the temperature increased with increasing PG content in the composites. This is a strong clue that the incorporation of PG enhanced the thermal stability of the composites. The ultimate temperature increased linearly with the applied voltage, and this made these composites good enough as temperature controllers for definite thermal exchange conditions around the heating devices.

Response of the PG/phenolic composites to gasoline gas

The dependence of the sensitivity (R_g/R_a) of the PG/resin composites on time to gasoline gas is depicted in Figure 9(a). The response time of the composites strongly depended on the PG volume fraction and morphology of the phenolic resin matrix. At low PG contents, gasoline gas could be slowly detected with a small amplitude, whereas with increasing PG concentration, the gasoline gas was rapidly detected with a high amplitude. There are two reasons for the slow detection of the gasoline gas. First, at a low graphite volume fraction, the PG particles were well wetted by the resin and formed a graphite gel (i.e., the graphite particles were encapsulated by the resin).[30] The graphite gel was hard to swell; this hampered the electrical response of the composites to the gasoline gas. Second, the gas molecules quickly diffused into the resin matrix and ruptured the conducting networks. This caused the response time with low PG contents to be lower than that with a high loading level. The SEM photograph of sample PG5 in Figure 9(b) reveals that the graphite particles were coated with resin, and there was weak interfacial adhesion between the graphite and resin matrix. In general, the PG/resin composites appear to be good candidates for gasoline gas detection.

Antistatic charge dissipation

To avoid electrostatic charging of an insulating matrix, an electrical conductivity greater than $\sigma = 10^{-6}$ $(\Omega\ \mathrm{cm})^{-1}$ is needed. The SE and dielectric constant as a function of the PG content are plotted in Figure 10(a).

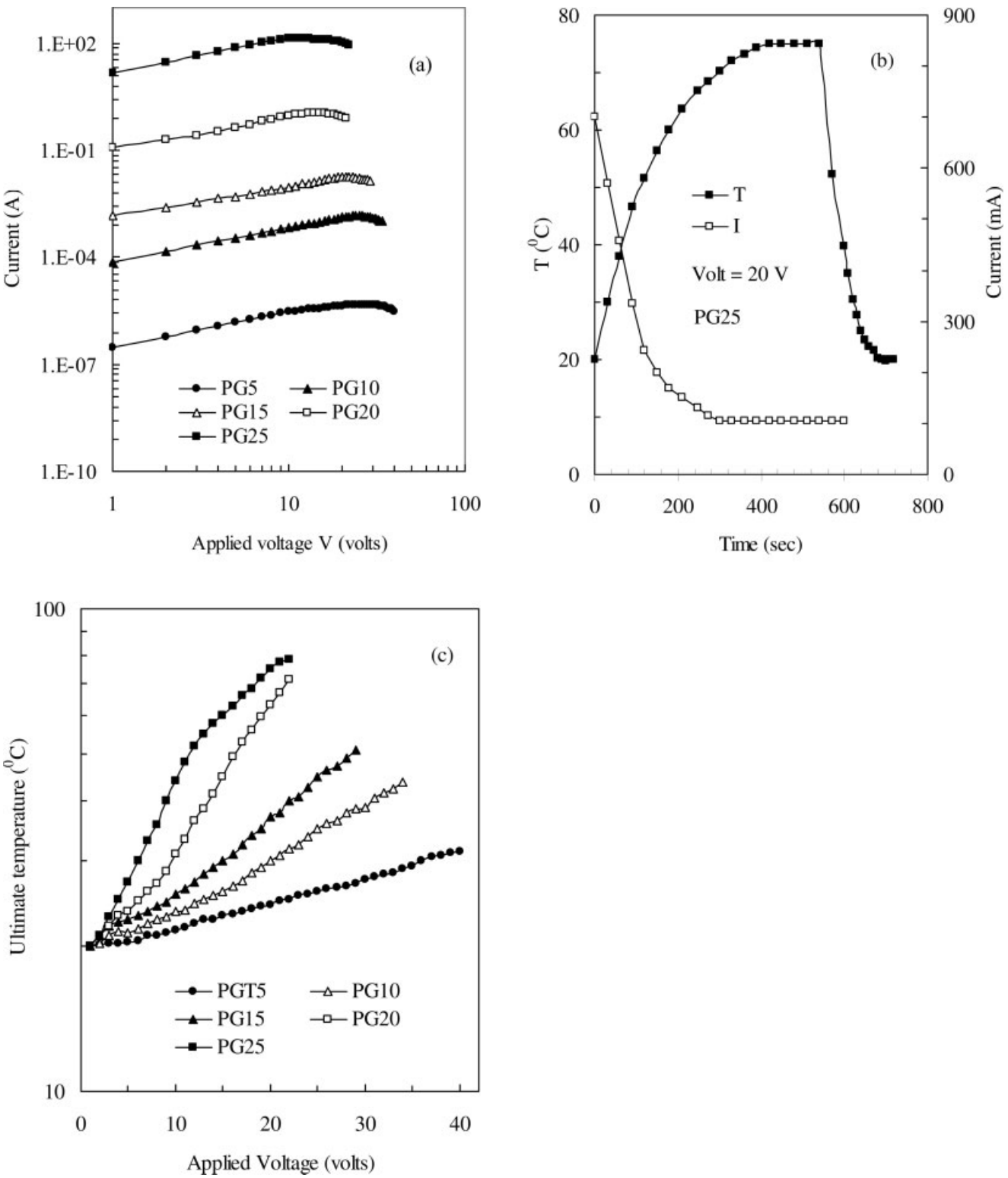

Figure 8 (a) Current–voltage characteristics of the PG/phenolic resin composites, (b) dependence of the ultimate temperature and current under an applied certain voltage for sample PG25, and (c) dependence of the maximum temperature of the bulk samples on the applied voltage of the PG/phenolic resin composites.

SE decreased, whereas the dielectric constant increased, with an increasing PG loading level in the composites. We believe that the static charge originated from the difference in the dielectric constants of the composites. A lower dielectric constant in the composites led to larger static charge generation. Because the composites generally displayed a lower dielectric constant at a low PG volume fraction, it would be pos-

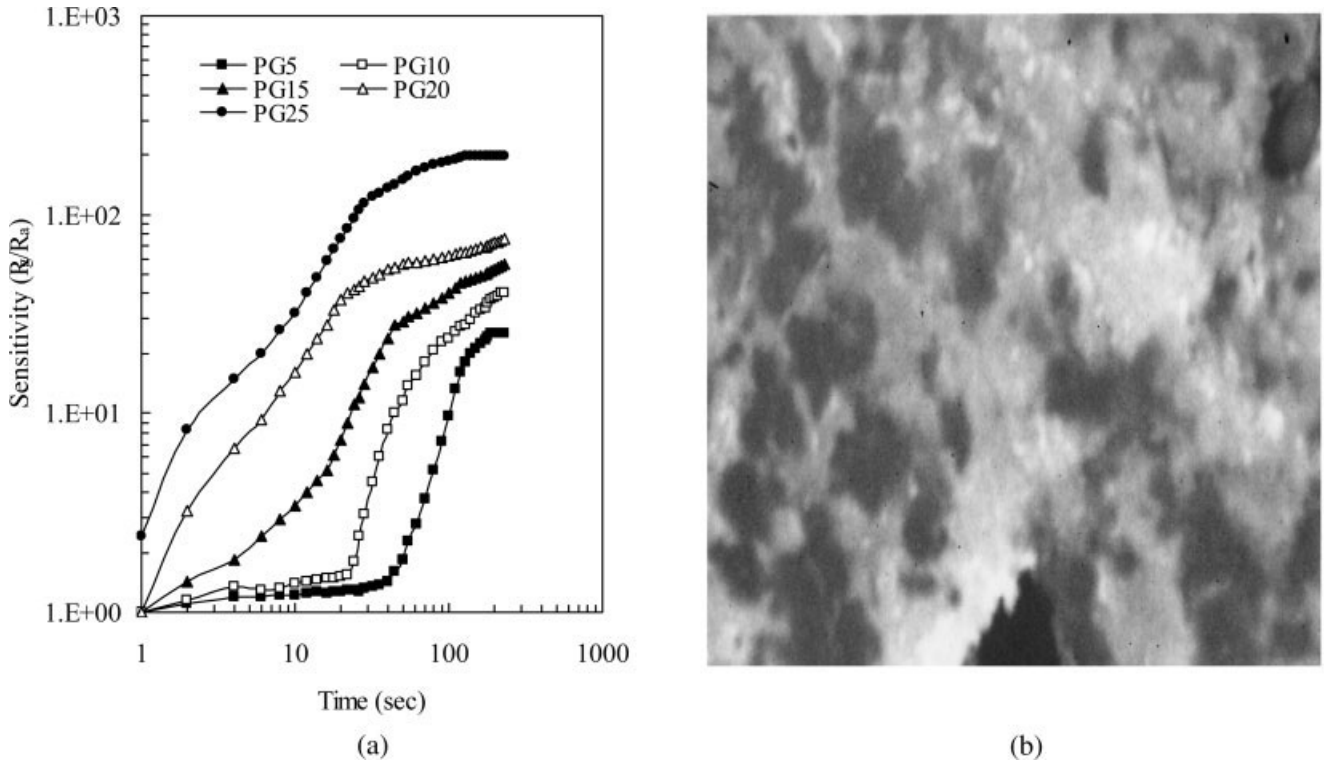

Figure 9 (a) Dependence of the sensitivity of the PG/resin composites immersed in gasoline gas on the time and (b) SEM of sample PG5 of the PG/resin composites.

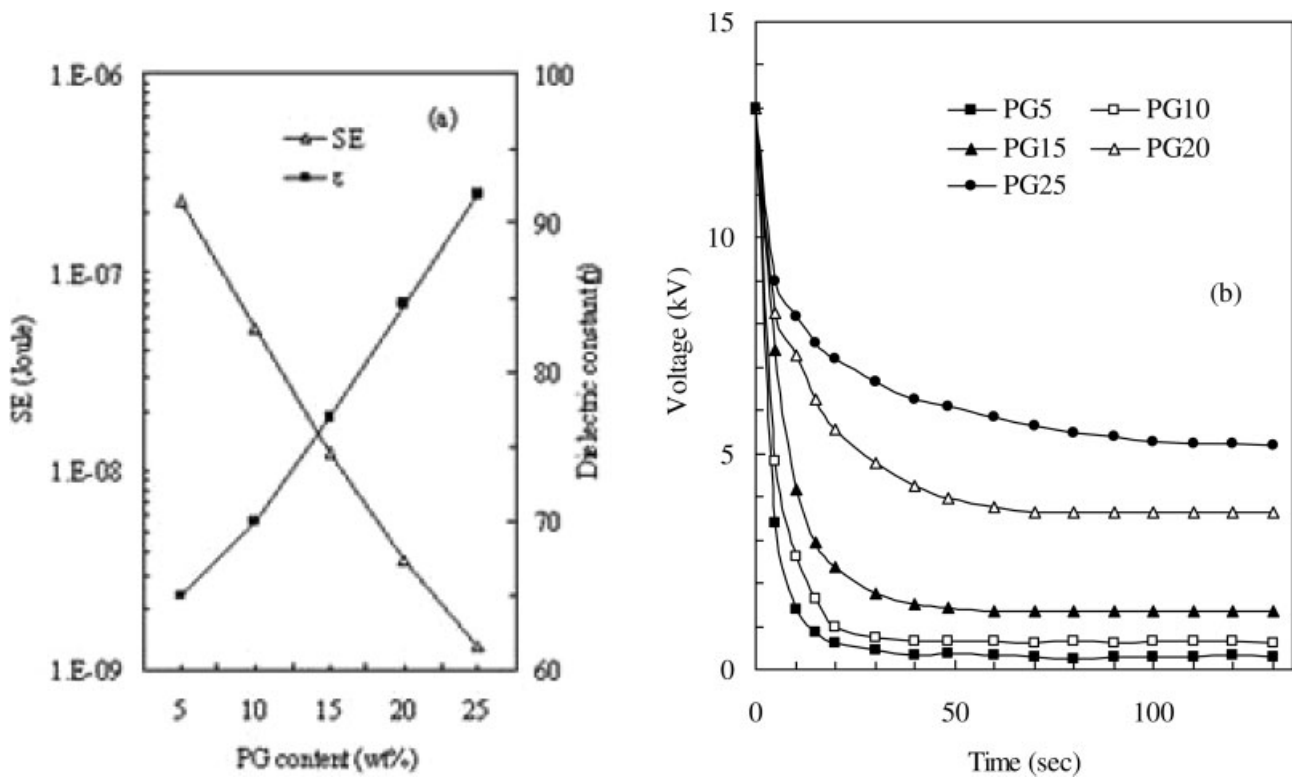

Figure 10 (a) SE and dielectric constant as functions of the PG content and (b) dependence of the decay voltage on the time under an applied voltage of about 13 kV.

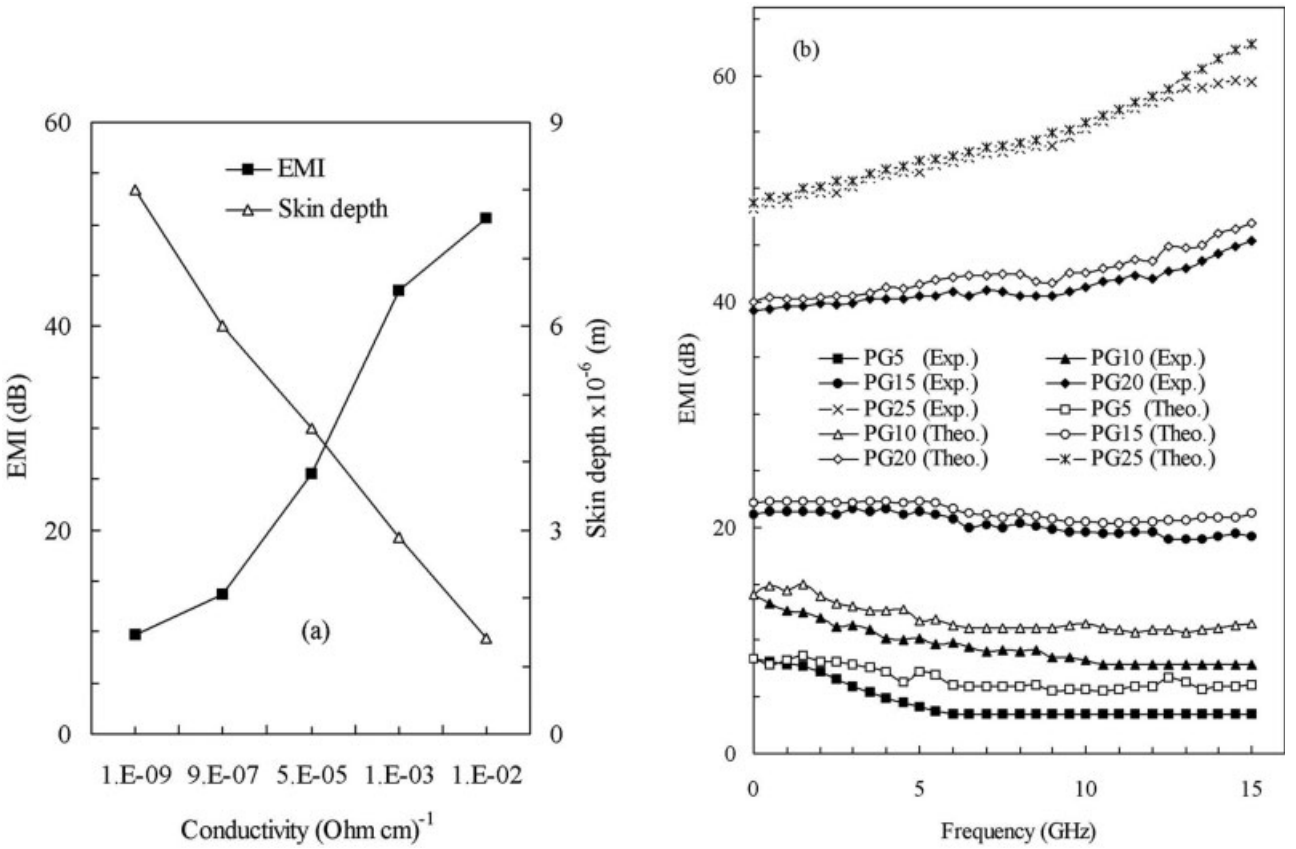

Figure 11 (a) EMI and δ against the graphite content for the phenolic resin composites and (b) experimental and calculated frequency dependence of EMI of the composites.

sible to eliminate the static electricity by a reduction of the dielectric constant of the composites. The dielectric constant increased as the PG content was raised. This was due to the interfacial polarization associated with graphite particles.[17] As the graphite content was raised, the graphite particles came into tighter contact, and clusters of the particles formed. The average interfacial polarization associated with a cluster was larger than that of an individual particle because of the increase in the dimensions of the conducting graphite inclusion. Therefore, the dielectric constant results were in agreement with the conductivity behavior described previously. Figure 10(b) shows the dependence of the decay voltage on time under an applied voltage of about 13 kV. The voltage reached steady-state values in less than 10 s for samples PG5, PG10, and PG15. This meant that at a lower volume fraction of PG, the composites could be very useful for charge-dissipation devices.

EMI shielding effectiveness

According to the near-field shielding theory, EMI can be described as follows:[25–31]

$$\mathrm{EMI} = 10\log\left[(0.25)\left\{\begin{array}{l}\left(\frac{\sigma}{2\varpi\varepsilon_0}\right)\left[\cosh\left(\frac{2d}{\delta}\right)-\cos\left(\frac{2d}{\delta}\right)\right] \\ +2\left(\frac{\sigma}{2\varpi\varepsilon_0}\right)^{\frac{1}{2}}\left[\sinh\left(\frac{2d}{\delta}\right)+\sin\left(\frac{2d}{\delta}\right)\right] \\ +2\left[\cosh\left(\frac{2d}{\delta}\right)+\cos\left(\frac{2d}{\delta}\right)\right]\end{array}\right\}\right] \quad (14)$$

where ϖ is the angular frequency and d is the sample thickness. δ is the skin depth of the material:

$$\delta = \frac{1}{\sqrt{\frac{\varpi}{2}\mu_r\sigma}} \quad (15)$$

where μ_r is equal to $4\pi \times 10^{-9}$ H/cm.

The effects of EMI and δ on the conductivity of the PG/resin composites are shown in Figure 11(a). With an increase in the PG loading, EMI increased, whereas δ decreased. This was ascribed to the fact that, with increasing PG content, the connectivity or interfacial adhesion between conductive phases became enough (i.e., tight contact) to allow the charge carriers to hop across the barriers within the resin matrix, and the conductivity increased sharply. This suggests that reflection dominates the shielding mechanism in composites.[1,8] The experimental EMI of the resin composites was compared with the theoretical EMI, as shown in Figure 11(b). The calculated values of EMI were higher than the measured results, particularly at a low loading level. This was attributed to the electromagnetic wave being absorbed within the resin matrix.[1] Our study indicated that sample PG25 offered shielding effectiveness of 62 dB at 13 GHz. The better shielding effectiveness at a high loading level of the PG/resin composites was attributed to a higher CLD and a closely packed structure, which was pore-free, as can be seen in SEM micrographs [Fig. 2(b)].

CONCLUSIONS

On the basis of the results and discussions, we can infer the following conclusions:

1. The inclusion of a plasticizer in the graphite/resin composites significantly affected the network structure of the composites. PG promoted the CLD, T_g, BR, γ, η, and enthalpy of the composites. Also, the plasticizer treatment of the graphite surface improved the mechanical properties of the composite samples because the plasticizer provided better interfacial adhesion of the graphite to the resin matrix.
2. The inclusion of PG, inducing chemical, structural, and morphological changes in the composites, resulted in the improvement of the electrical conductivity and led to a lower percolation threshold. Temperature–resistivity analysis confirmed that the PTCρ effect of the PG/resin composite thermistors originated from the increase in both the bulk expansion and grain boundaries.
3. The current and voltage of the composites showed a switching effect, which could make them very useful for current switching in electronic devices. Furthermore, the temperature increased linearly with the applied voltage of the composites, and this could make these composites quite useful for temperature control.
4. The PG/phenolic composites with high PG contents had high sensitivity to gasoline gas.
5. The static charge was eliminated at a low loading level of PG in the phenolic composites and with a lower dielectric constant of the composites.
6. The EMI properties of the resin composites varied with the PG/resin ratio and exhibited a high EMI value of about 62 dB at a high loading level. These composites are most promising for EMI shielding because of their light weight, which is of critical importance in aerospace applications and corrosion resistance and for ease of processing.

References

1. El-Tantawy, F.; Kamada, K.; Ohnabe, H. J Appl Polym Sci 2003, 97, 87.
2. Chen, G.; Weng, W.; Wu, D.; Wu, C. Eur Polym J 2003, 39, 2329.
3. Chen, G.; Wu, D.; Weng, W.; Yan, W. J Appl Polym Sci 2001, 82, 2506.
4. Chen, G.; Wu, D.; Weng, W.; Yan, W. Polym Eng Sci 2001, 41, 2148.
5. Chen, G.; Weng, W.; Dajun, W.; Cuiling, W. J Polym Sci Part B: Polym Phys 2004, 42, 155.
6. Chen, G.; Weng, W.; Dajun, W. Polymer 2003, 44, 8119.
7. Krupa, I.; Novak, I.; Chodak, I. Synth Met 2004, 145, 245.
8. Wang, W. P.; Pan, C. Y. Polymer 2004, 45, 3987.
9. Huang, C. Y.; Mo, W.; Roan, M. Surf Coat Technol 2004, 184, 123.
10. Dradhan, D. K.; Samantaray, B. K.; Choudhary, R. J Power Sources 2005, 139, 384.
11. Hang, Z.; Longtu, L.; Zhilum, G. Sens Actuators A 2001, 5, 3108.
12. Lee, B.; Kim, M. S. Macromol Mater Eng 2001, 286, 114.
13. Hyung, D. C.; Chan, W. S. J Appl Polym Sci 1999, 72, 75.
14. Mihai, R.; Nicoleta, S.; Daniela, R. Polym Test 2001, 20, 409.
15. Wan, J. L.; Yong, J. K.; Shinyoung, K. Synth Met 2000, 113, 237.
16. Chi, Y. H.; Chang, C. W. Eur Polym J 2000, 36, 2729.
17. Chen, X.; Jiang, Y.; Zhiming, W.; Dan, L.; Yang, J. Sens Actuators B 2000, 66, 37.
18. Das, N. C.; Khastgir, D.; Chaki, T. K.; Chakraborty, A. Compos A 2000, 31, 1069.
19. Sandler, J.; Shaffer, M. S. P.; Prasse, T.; Bauhofer, W.; Schulte, K. Polymer 1999, 40, 5967.
20. Sack, H. S.; Moriarity, M. C. Solid State Commun 1995, 3, 93.
21. Xiao, S. Y.; Lie, S.; Yi, P. Compos Sci Technol 2001, 61, 949.
22. Cespeds, F.; Fabregas, E. M.; Alegret, A. Anal Chem 1996, 15, 296.
23. Jia, W.; Tchoudakov, R.; Segal, E.; Joseph, R.; Narkis, M.; Siegmann, A. Synth Met 2003, 132, 269.

24. Fournier, J.; Boiteux, G.; Seytre, G.; Marichy, G. Synth Met 1996, 84, 839.
25. Vishal, S.; Tiwari, A. N.; Kulkarni, A. R. Mater Sci Eng B 1996, 41, 310.
26. Lee, C. Y.; Lee, D. E.; Joo, J.; Kim, M. S.; Lee, J. Y.; Jeong, S. H.; Byun, S. W. Synth Met 2001, 119, 429.
27. Pomposo, J. A.; Rodriguez, J.; Grande, H. Synth Met 1999, 104, 107.
28. Lee, C. Y.; Song, H. G.; Jang, K. S.; Oh, J.; Epsten, A. J.; Joo, J. Synth Met 1999, 102, 1349.
29. Yuping, D.; Shunhua, L.; Hongtao, G. Sci Technol Adv Mater 2005, 6, 1.
30. Wang, Y.; Jing, X. Polym Adv Technol 2005, 16, 344.
31. Sperling, L. H. Physical Polymer Science; Wiley: New York, 2001.
32. Leo, C. J.; Subbarao, G. V.; Chowdari, B. V. R. Solid State Ionics 2002, 148, 159.